ATLAS NOTE

ATLAS-CONF-2011-135

August 21, 2011

Update of the Combination of Higgs Boson Searches in 1.0 to 2.3 fb^{-1} of pp Collisions Data Taken at $\sqrt{s} = 7$ TeV with the ATLAS Experiment at the LHC

The ATLAS collaboration

Abstract

The combination of searches for the Higgs boson by the ATLAS experiment with the first $\sim$1 fb^{-1} of data taken in 2011 at the LHC is updated. The $H \to ZZ^{(*)} \to \ell^+\ell^-\ell^+\ell^-$ and $H \to WW^{(*)} \to \ell^+\nu\ell^-\overline{\nu}$ searches are complemented with additional datasets corresponding to 1.1 and 0.6 fb^{-1} of integrated luminosity and now correspond to 2–2.3 fb^{-1}and 1.7 fb^{-1} respectively. The $H \to WW^{(*)} \to \ell^+\nu\ell^-\overline{\nu}$ channel is improved and two channels searching for the Higgs boson decaying to tau leptons are now included. An excess of events is observed in the low mass range. Its significance is at most approximately 2 standard deviations above the expected SM background. The Higgs boson mass ranges from 146 GeV to 232 GeV, 256 GeV to 282 GeV and 296 GeV to 466 GeV are excluded at the 95% CL, while the expected Higgs boson mass exclusion in the absence of a signal ranges from 131 GeV to 447 GeV. The result of these searches is also interpreted in the framework of a Standard Model with the addition of a heavy sequential fourth generation of fermions. In this model Higgs boson masses above 120 GeV and up to 600 GeV are excluded at the 95% CL.

This note presents an update of the combination of searches for the Higgs boson [1–6] by the ATLAS experiment reported in Ref. [7] with data taken in 2011 at the LHC using a dataset corresponding to an integrated luminosity ranging from 1.0 to 1.2 fb^{-1} of pp collisions at a centre-of-mass energy of 7 TeV. In this note only changes with respect to the combination of Ref. [7] are reported. For this update the $H \to ZZ^{(*)} \to \ell^+\ell^-\ell^+\ell^-$ and $H \to WW^{(*)} \to \ell^+\nu\ell^-\overline{\nu}$ searches are complemented with additional datasets corresponding to up to 1.1 and 0.6 fb^{-1} of integrated luminosity respectively, the $H \to WW^{(*)} \to \ell^+\nu\ell^-\overline{\nu}$ analysis is updated and two new channels of inclusive searches for Higgs decays in a pair of tau leptons are included in the combination. The $H \to \gamma\gamma$, $H \to ZZ \to \ell^+\ell^-\nu\overline{\nu}$, $H \to ZZ \to \ell^+\ell^- q\overline{q}$, $WH \to \ell\nu b\overline{b}$ and $ZH \to \ell\ell b\overline{b}$ are unchanged with respect to [7], except for the separation of cross section uncertainties to comply with the standard procedure agreed upon in Ref. [8]. The latter modification has not been completed in time for the $\ell\nu q\overline{q'}$ channel inputs, which are removed from this combination update. The details of the individual analyses can be found in their respective references [9–16].

The recent additional data used to update the $H \to ZZ^{(*)} \to \ell^+\ell^-\ell^+\ell^-$ and $H \to WW^{(*)} \to \ell^+\nu\ell^-\overline{\nu}$ searches in this combination were taken in conditions similar to those of the previous combination except for the higher average number of additional pile-up events. These changes have been studied in detail, their impact on the analyses has been taken into account and reported in this note where relevant.

Only the features relevant to the combination of the two new channels and the updates of the $H \to WW^{(*)} \to \ell^+\nu\ell^-\overline{\nu}$ are recalled here. In the following a lepton ℓ denotes an electron or a muon.

- $H \to ZZ^{(*)} \to \ell^+\ell^-\ell^+\ell^-$ update: This analysis was updated to include 2.0-2.3 fb^{-1} of data with no change in the analysis selections. Six new candidates were observed in addition to the 18 reported previously, none of them contributing significantly to regions previously having an excess of events.

- $H \to WW^{(*)} \to \ell^+\nu\ell^-\overline{\nu}$ update: The new event selection uses an improved b-tagging algorithm [17] allowing for a more efficient b-jet veto. It is also globally reoptimised in the high mass region (above 220 GeV) taking into account the impact of the precision of the background estimates in the control regions. A minor improvement is that the tau polarization is now taken into account in the simulation of the background processes (such as WW, $t\bar{t}$ and Z+$jets$ production). While the previous data showed an excess at low mass in this channel, it is worth noting that the new data is compatible with the background-only hypothesis.

- $H \to \tau\tau \to \ell\tau_{had}3\nu$: The event selection in this analysis requires one lepton (ℓ) (with transverse momentum in excess of 20 GeV for muons and 25 GeV for electrons) from a fully leptonic tau decay, an oppositely charged tau candidate τ_{had} with transverse momentum larger than 20 GeV, selected using a calorimeter jet associated to one or three tracks and a missing transverse energy larger than 20 GeV due to the three undetected neutrinos. Events with an additional lepton are removed to suppress the $Z/\gamma^* \to \ell^+\ell^-$ and $t\bar{t}$ background processes. Finally, to suppress the $W \to \ell\nu$ background process, the transverse mass of the lepton and missing energy system is required to be smaller than 30 GeV. An important aspect of this analysis is the use of a new reconstruction technique to estimate the invariant mass of the pair of tau leptons, which does not assume a strict collinearity between the visible and invisible decay products of the tau leptons [18]. The main background in this analysis is the $Z/\gamma^* \to \tau^+\tau^-$ process. Its invariant mass shape is estimated using an embedding technique where muons from Z decay events are substituted by simulated tau decays. The other backgrounds are in part estimated using same sign events and in part using the Monte Carlo for the difference between the number of opposite sign and same sign events. The individual 95% CL limit on the cross section normalised to the Standard Model Higgs boson cross section, as functions of the Higgs boson mass for this channel is illustrated in Fig. 8(a) of Appendix A.

- $H \to \tau\tau \to \ell^+\ell^- + 4\nu$: In this event-counting analysis the presence of two leptons with with transverse momentum in excess of 10 GeV for muons and 15 GeV for electrons is required. One of these is required to have higher momentum in order to trigger the event, and a jet with transverse momentum in excess of 40 GeV is required. As a consequence of the boost of the Higgs boson, the enhanced transverse momentum of the Higgs decay products among which, four are neutrinos, implies a larger $E_{\mathrm{T}}^{\mathrm{miss}}$ in the event. The large $E_{\mathrm{T}}^{\mathrm{miss}}$ and high jet transverse momentum allows for a good discrimination against background processes such as $\mathrm{Z}/\gamma^* \to \ell\ell$ and QCD. The $\mathrm{Z} \to \ell\ell$ background is further reduced when the two leptons are of the same flavor by requiring the dilepton invariant mass to be substantially smaller than the mass of the Z. Requiring at least one high p_{T} jet also significantly reduces the $\mathrm{Z} \to \tau\tau$ background while the effect of this cut on the signal is small, due to the large fraction of Vector Boson Fusion (VBF) events and the expected larger radiation in the initial state for the gluon-fusion production process, the Z being mainly produced by quarks in the initial state. The boost of the Higgs also increases the efficiency of the cut on the fractions of undetected momentum in the collinear approximation [9], which are in turn important to define the kinematic selection. The main backgrounds are the Z decays to a pair of tau leptons and top-quark pair production. The former is estimated using the same embedding technique as that used in the $H \to \tau\tau \to \ell\tau_{had}3\nu$ channel. The latter and all other backgrounds except for the QCD events with jets faking leptons (comprised of Z decays to two electrons or muons, single top, and diboson production) are taken from simulation. The fake lepton QCD background is estimated in an independent control sample. The individual 95% CL limits on the cross section, normalised to the Standard Model Higgs boson cross section, as functions of the Higgs boson mass for this channel are illustrated in Fig. 8(a) of Appendix A.

Table 1: Summary of the updates compared to Ref. [7], including the luminosities used, analysis optimisation (Analysis Opt.) and references for each channel included in this combination.

	$H \to \tau^+\tau^-$				$H \to WW^{(*)}$		$H \to ZZ^{(*)}$		
	$\tau_\ell\tau_{had}$	$\tau_\ell\tau_\ell + jet$	$H \to \gamma\gamma$	$H \to b\bar{b}$	$\ell\nu\ell\nu$ 0-jet	$\ell\nu\ell\nu$ 1-jet	$\ell\ell\ell\ell$	$\ell\ell\nu\nu$	$\ell\ell qq$
$\mathscr{L}$ (fb^{-1}) Old	1.06	1.06	1.08	1.04	1.04		1.04-1.21	1.04	1.04
$\mathscr{L}$ (fb^{-1}) New	1.06	1.06	1.08	1.04	1.70		1.96-2.28	1.04	1.04
Analysis Opt.	No	No	No	No	Yes		No	No	No
Reference	[9]	[10]	[11]	[12]	[13]		[14]	[15]	[16]

A synoptic summary of the changes in luminosities and analysis for this combination with respect to the combination of Ref. [7] is reported in Table 1. The numbers of observed events and expected signal and background events for all channels are summarised in Table 2, and the distribution of the final discriminants can be seen in Figs. 1 and 2. To illustrate the relative strength of each channel these numbers are given in an interval containing $\sim 90\%$ of the signal around the most probable value of the invariant or transverse mass distributions, except for the $H \to WW^{(*)} \to \ell^+\nu\ell^-\overline{\nu}$ and $H \to \tau\tau \to \ell^+\ell^- + 4\nu$ channels, which are event-counting analyses. For most channels where the invariant or transverse mass is used as discriminant, the fit performed uses more information than is presented here. The precise sensitivity of the analyses can therefore not be deduced from these numbers.

The correlated systematic uncertainties are unchanged. All additional systematic uncertainties are uncorrelated, corresponding either to background estimates or to the tau identification efficiency, which affects only the $H \to \tau\tau \to \ell\tau_{had}3\nu$ channel and amounts to $\pm 9.1\%$. The tau energy scale is fully

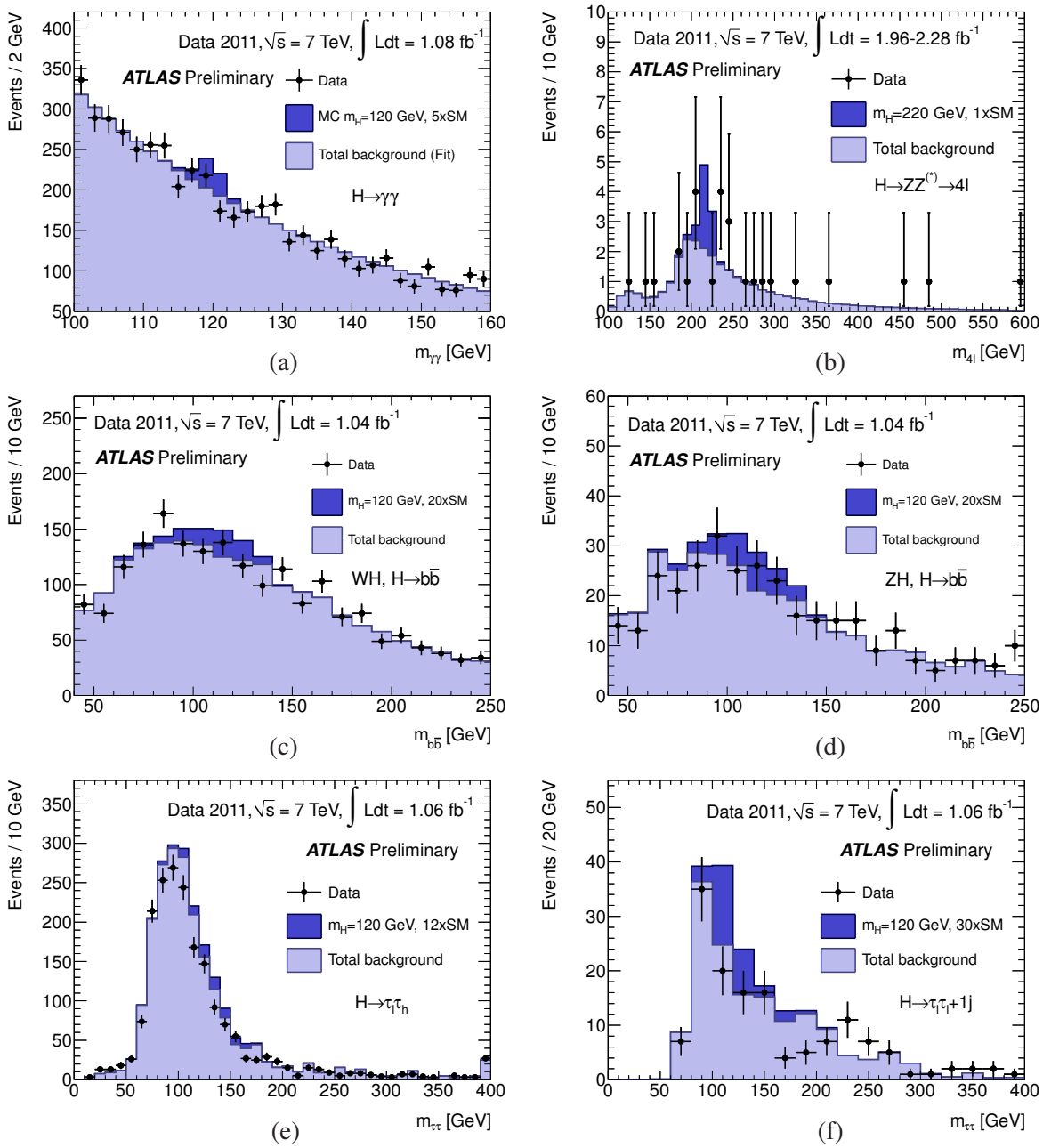

Figure 1: The invariant mass distributions for the candidate events selected, the total background and the signal expected in the $H \to \gamma\gamma$ (a), $H \to ZZ^{(*)} \to \ell^+\ell^-\ell^+\ell^-$ (b), the $WH \to \ell\nu b\bar{b}$ (c) and $ZH \to \ell^+\ell^- b\bar{b}$ (d), and the $H \to \tau\tau \to \ell\tau_{had}3\nu$ (e) and $H \to \tau\tau \to \ell^+\ell^- + 4\nu$ (f) channels. The Higgs boson mass hypothesis used to illustrate the signal and the multiplicative factor applied to its normalisation are indicated in each legend. For the $H \to ZZ^{(*)} \to \ell^+\ell^-\ell^+\ell^-$ channel asymmetric error bars representing 68.3% central confidence intervals are used.

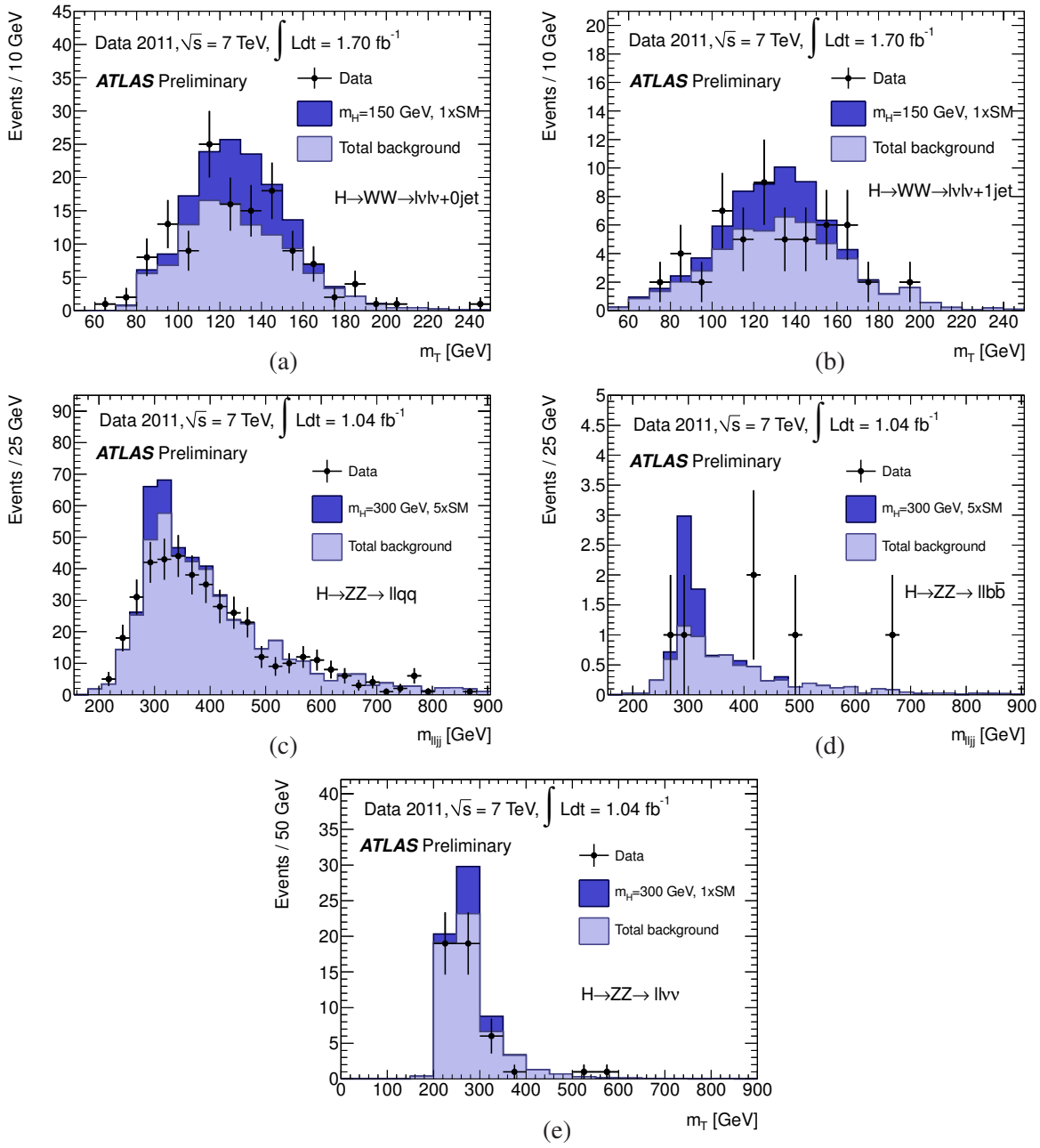

Figure 2: The invariant or transverse mass distributions for the candidate events selected, the total background and the signal expected in the $H \to WW^{(*)} \to \ell^+\nu\ell^-\overline{\nu}$ zero jet (a) and one jet (b) channels, the $H \to ZZ \to \ell^+\ell^- q\overline{q}$ untagged (c) and tagged (d) categories and the $H \to ZZ \to \ell^+\ell^-\nu\overline{\nu}$ (e) channel. The Higgs boson mass hypothesis used to illustrate the signal and the multiplicative factor applied to its normalisation are indicated in each legend.

Table 2: Numbers of observed events and the expected numbers of signal and background events in the channels used in the combination. For all channels except $H \to WW^{(*)} \to \ell^+\nu\ell^-\overline{\nu}$ and $H \to \tau\tau \to \ell^+\ell^- + 4\nu$ these numbers are estimated in an interval containing $\sim 90\%$ of the signal around the most probable value of the invariant or transverse mass distributions. These numbers are for information only as the analyses typically fit the distributions.

	$H \to \tau^+\tau^-$		$H \to \gamma\gamma$	$H \to b\bar{b}$	$H \to WW^{(*)}$ $\ell\nu\ell\nu$		$H \to ZZ^{(*)}$		
	$\tau_\ell\tau_{had}$	$\tau_\ell\tau_\ell + jet$			0-jet	1-jet	$\ell\ell\ell\ell$	$\ell\ell\nu\nu$	$\ell\ell qq$
				m_H=120 GeV					
s	8.0	0.8	15.9	5.5	3.9	1.4	0.2	-	-
b	1218	47.1	723	992	36.5	12.9	0.6	-	-
N_{obs}	1072	46	787	1131	47	14	0	-	-
				m_H=150 GeV					
s	-	-	6.9	-	33.8	11.9	2.0	-	-
b	-	-	416	-	53.4	23.4	0.6	-	-
N_{obs}	-	-	405	-	70	23	1	-	-
				m_H=200 GeV					
s	-	-	-	-	13.9	6.5	5.2	4.5	31.4
b	-	-	-	-	39.6	25.1	5.7	62.0	7433
N_{obs}	-	-	-	-	36	28	5	54	7225
				m_H=300 GeV					
s	-	-	-	-	11.3	7.1	3.3	9.1	6.8
b	-	-	-	-	120.6	76.3	4.5	42.3	195
N_{obs}	-	-	-	-	130	78	4	38	200
				m_H=400 GeV					
s	-	-	-	-	-	-	2.3	9.0	9.8
b	-	-	-	-	-	-	4.1	33.1	207
N_{obs}	-	-	-	-	-	-	2	45	239

correlated with the Jet Energy Scale and thus does not require a separate treatment.

The correlated detector-related systematic uncertainties are classified in the five following generic categories: the electron-photon-related (i) and muon-related (ii) systematic uncertainties including identification, energy scale and energy resolution; the Jet Energy Scale (JES) and Jet Energy resolution (JER) (iii) with a special treatment of the b-jet energy scale; the MET-related (iv) systematic uncertainty, which is in a large part correlated to (iii); and the systematic uncertainties related to the b-tagging and associated veto (v). These sources of systematic uncertainties are considered as 100% correlated among channels. They are discussed in more detail in Ref. [7] and the references of each individual channel [9–16, 19, 20].

The Higgs boson production cross sections are computed to up to next-to-next-to-leading order (NNLO) in QCD for the gluon fusion ($gg \to H$), vector boson fusion ($qq' \to qq'H$) and associated WH/ZH production processes ($q\bar{q} \to WH/ZH$) and to next-to-leading order (NLO) for the associated production with a $t\bar{t}$ pair ($q\bar{q}/gg \to t\bar{t}H$). These cross sections and decay branching ratios and their related uncertainties are compiled in Ref. [21]. The scale uncertainties amount to $^{+12}_{-7}$% for the $gg \to H$ process, ± 1% for the $qq' \to qq'H$ and associated WH/ZH processes, and $^{+4}_{-1}$% for the $q\bar{q}/gg \to t\bar{t}H$ process. The uncertainties related to the Parton Distribution Functions (PDF) amount to ± 8% for the predominantly gluon-initiated processes $gg \to H$ and $q\bar{q}/gg \to t\bar{t}H$, and ± 4% for the predominantly quark-initiated $qq' \to qq'H$ and WH/ZH processes [22]. The PDF uncertainties are assumed to be 100% correlated among processes with identical initial states, regardless of these being signal or background. The theoretical uncertainty associated with the exclusive Higgs production processes with one additional jet in the $H \to WW^{(*)} \to \ell^+\nu\ell^-\overline{\nu}$ channel amounts to ± 20% and is treated according to the prescription of Ref. [8].

The Monte Carlo generators used in the updated and additional channels are the same as those used in Ref. [7] and the treatment of correlations between Monte Carlo background normalisations, scale factors or shapes estimates are unchanged.

The effect on the signal yield in each channel of the major sources of systematic uncertainty is summarised in Table 3.

Table 3: Main correlated systematic uncertainties used in the analysis. These relative uncertainties (%) correspond to the overall effect on the per-event signal efficiency of the $\pm 1\sigma$ variation of the source of systematic uncertainty. Some of them, such as the energy scale in the $H \to \gamma\gamma$ search, are included but are not apparent in this table as they do not affect event rates.

	$H \to \tau^+\tau^-$		$H \to \gamma\gamma$	$H \to b\bar{b}$	$H \to WW^{(*)}$	$H \to ZZ^{(*)}$		
	$\tau_\ell\tau_{had}$	$\tau_\ell\tau_\ell + jet$			$\ell\nu\ell\nu$	$\ell\ell\ell\ell$	$\ell\ell\nu\nu$	$\ell\ell qq$
Luminosity	± 3.7	± 3.7	± 3.7	± 3.7	± 3.7	± 3.7	± 3.7	± 3.7
e/γ eff.	± 3.5	$^{+2.0}_{-2.1}$	$^{+11.6}_{-10.4}$	± 2.3	± 2.2	± 3.3	± 1.2	± 1.1
e/γ E. scale	$^{+1.3}_{-0.1}$	$^{+0.2}_{-0.5}$	-	$^{+1.5}_{-1.6}$	± 0.1	-	$^{+0.8}_{-1.1}$	-
e/γ res.	-	± 3.7	-	$^{+2.1}_{-1.5}$	± 0.1	-	-	-
μ eff.	± 1.0	$^{+2.0}_{-2.1}$	-	$^{+1.1}_{-2.0}$	± 0.6	± 1.2	$^{+0.8}_{-0.7}$	± 0.6
μ res.	-	$^{+0.4}_{-0.6}$	-	± 5.8	± 1.6	-	-	-
Jet/τ/MET E. scale	$^{+19}_{-16}$	$^{+3.3}_{-10.0}$	-	$^{+21}_{-17}$	± 6.1	-	$^{+5.9}_{-4.0}$	$^{+3.7}_{-10.4}$
JER	-	± 2.0	-	± 2.5	$^{+2.2}_{-1.8}$	-	-	$^{+2.1}_{-0.0}$
MET	-	$^{+4.4}_{-5.3}$	-	$^{+5.5}_{-6.1}$	-	± 0.6	$^{+6.6}_{-4.2}$	-
b-tag eff.	-	-	-	$^{+37}_{-33}$	± 0.1	-	$^{+4.3}_{-4.4}$	-

The combination procedure follows precisely that described in Refs. [7, 8, 19]. It is based on the profile likelihood test statistic [23]. The 95% CL cross section limits in units of the Standard Model expectation set by the individual channels and the combination of the $H \to \tau\tau \to \ell\tau_{had}3\nu$ and $H \to \tau\tau \to \ell^+\ell^- + 4\nu$ channels using the CL_s prescription [24,25] are shown in Fig. 3. The combination of all channels is shown in Figs. 4(a) and 4(b) in terms of the observed and the expected upper limit at a 95% CL on the excluded Higgs boson production cross section, normalised to the Standard Model value. Full numerical details can be found in Table 4 of Appendix B. The limits shown are made using the asymptotic approximation [23], which has been verified using Monte Carlo experiments and a Bayesian calculation, which agrees with these results to within a few percent [7]. The expected exclusion covers the Standard Model Higgs boson mass range from 131 GeV to 447 GeV. The observed 95% CL exclusion regions are from 146 GeV to 232 GeV, 256 GeV to 282 GeV and 296 GeV to 466 GeV. A deficit of events observed in the excluded mass range and in particular between 300 to 400 GeV as reported in Ref. [7] is unchanged and still due to the concordance of various small deficits in several high mass channels. The observed limit is in good agreement with the background only expectation over most of the available range in Higgs boson mass hypotheses, except in the low mass range (from $\sim$ 130 GeV up to $\sim$ 170 GeV), range where a slight excess is still observed.

The consistency with the background-only hypothesis is estimated by the p_0 probability that a background-only experiment is more signal-like than the observed one. The probability p_0 is bounded to be equal to 50% for downward fluctuations of the background and smaller than 50% when an excess of events is observed. This probability is displayed as a function of the Higgs boson mass hypothesis in Figs. 5(a) and 5(b). There were three excesses of events reported in Ref. [7]. The first excess, peaking at a Higgs boson mass hypothesis of 127 GeV, was due to the combined effect of a broad excess of events in the $H \to WW^{(*)} \to \ell^+\nu\ell^-\overline{\nu}$ channel and an excess in the $H \to \gamma\gamma$ channel. As reported in Ref. [13] the latter excess in the updated $H \to WW^{(*)} \to \ell^+\nu\ell^-\overline{\nu}$ analysis is less significant. This first excess is as a consequence also less significant. The second was peaking at a Higgs boson mass hypothesis of 245 GeV. It was not very significant ($\sim 2\sigma$) and was due essentially to an accumulation of events in the $H \to ZZ^{(*)} \to \ell^+\ell^-\ell^+\ell^-$ analysis. The significance of this excess has decreased with the additional data. Finally the third corresponded to the most extreme value of the p_0, which was observed at 144 GeV and resulted from the excess in the $H \to WW^{(*)} \to \ell^+\nu\ell^-\overline{\nu}$ channel and one event observed in the $H \to ZZ^{(*)} \to \ell^+\ell^-\ell^+\ell^-$ analysis. The significance of this excess was 2.8σ, and the probability of such an excess in the range studied was estimated to be approximately 10%. The excess is still observed, but mainly because of the less significant broad excess in the $H \to WW^{(*)} \to \ell^+\nu\ell^-\overline{\nu}$ analysis, its significance has decreased to 2σ, corresponding to a probability of a background fluctuation at the percent level. This probability is the so-called *local* probability of a background fluctuation. The approximate trial factor or *Look Elsewhere Effect* computation described in Refs. [8,26] does not apply in cases where the *local* probability is at the percent level. Given the global probability of approximately 10% for the most significant excess reported in Ref. [7], the fluctuation observed here is highly likely. The overall consistency of these excesses with an expected signal is shown in Figs. 5(a) and 5(b) where the expected p_0 in presence of a Standard Model signal is displayed.

The significance with which the Standard Model Higgs boson is excluded is shown in Fig. 6(a) and 6(b). It can be noted that a signal of the Standard Model strength is excluded at high confidence for 360 GeV, while an exclusion Confidence Level (CL_s) in excess of 99% is observed in the regions between 160 GeV and 220 GeV and between 300 GeV and 420 GeV. At an exclusion level of 90% the picture is not very different from the 95% level used herein.

The searches for the Standard Model Higgs boson can also be interpreted in the framework of a Standard Model with a fourth generation of heavy fermions. The masses of the fourth-generation leptons and down-type quark are set to a high value of 600 GeV. The mass difference between the fourth generation up-type and down-type quarks is fixed to $50 + 10 \times ln(m_H/115[GeV])$ for consistency with

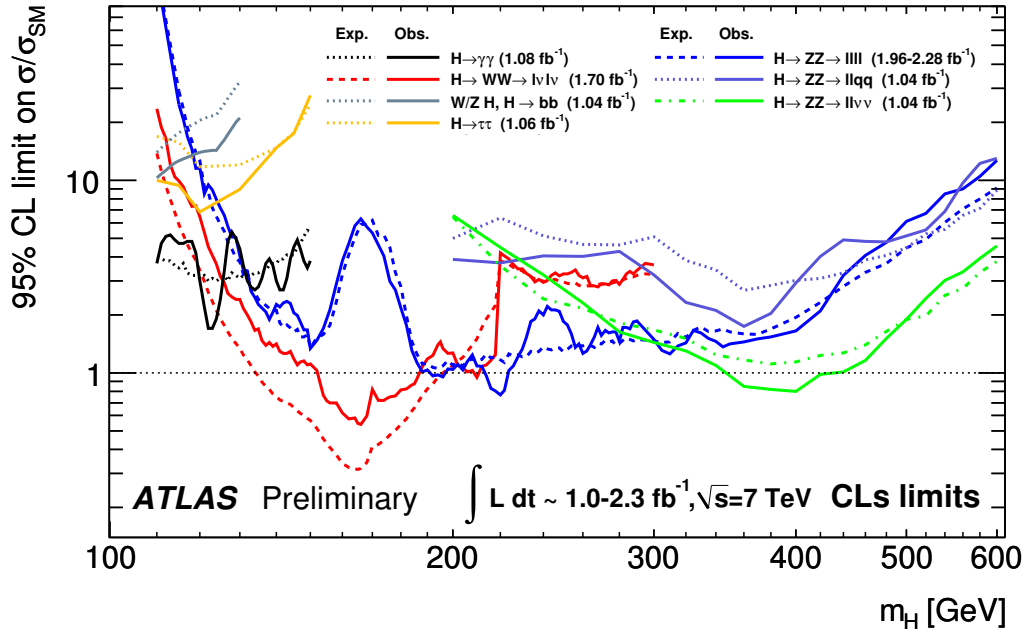

Figure 3: The expected (dashed) and observed (solid) cross section limits for the individual search channels, normalised to the Standard Model Higgs boson cross section, as functions of the Higgs boson mass. These results use the profile likelihood technique with 95% CL limits using the CL_S construction.

the electroweak precision measurements [27]. The systematic uncertainties related to the QCD scale, PDF and α_S uncertainties are assumed to be the same as the Standard Model case for the gluon fusion process. To account for the missing electroweak radiative corrections, which can have a sizable impact on the production cross section, an additional $\pm 10\%$ systematic uncertainty is added linearly to the overall theoretical uncertainty on the production cross section. The impact of a heavy fourth generation of fermions on the signal production rates in the various channels are not homogeneous, for a reinterpretation of the searches for the Standard Model Higgs boson in this framework a specific combination is therefore necessary. The result of this combination is illustrated in Fig. 7. With the aforementioned set of model parameters, Higgs boson mass hypotheses above 116 GeV are expected to be excluded at the 95% CL and a Higgs boson with mass in excess of 120 GeV and up to 600 GeV is excluded at the 95% CL. Previous exclusion limits in this framework, set by Tevatron and LHC experiments, are reported in [19, 28, 29].

Conclusion

The outstanding performance of the LHC, that allowed more than 1 fb^{-1} of integrated luminosity to be accumulated by the end of June of this year, exceeding the objective of the LHC for 2011, has continued throughout the summer, allowing for additional datasets corresponding to 0.6 and up to 1.1 fb^{-1} of integrated luminosity to be added to the $H \to WW^{(*)} \to \ell^+\nu\ell^-\overline{\nu}$ and $H \to ZZ^{(*)} \to \ell^+\ell^-\ell^+\ell^-$ channels respectively, extending the total dataset to up to 2.3 fb^{-1}. The $H \to WW^{(*)} \to \ell^+\nu\ell^-\overline{\nu}$ channel has also been updated, mostly with an improved b-tagging algorithm. Two less sensitive channels in the low Higgs boson mass hypotheses range, $H \to \tau\tau \to \ell\tau_{had}3\nu$ and $H \to \tau\tau \to \ell^+\ell^- + 4\nu$, using 1.1 fb^{-1} of data, have been added to the combination.

The Standard Model Higgs boson exclusion at 95% CL has been widened to Higgs boson mass

hypotheses in the ranges from 146 GeV to 232 GeV, 256 GeV to 282 GeV and 296 GeV to 466 GeV, extending the limits set by previous measurements and in agreement with the sensitivity of this search. The exclusion Confidence Level (CL_s) is about 99% in the region between 160 GeV and 220 GeV and exceeds 99% between 300 GeV and 420 GeV. These analyses have also been interpreted in the framework of the Standard Model with the addition of a fourth generation of fermions, excluding a Higgs boson with mass above 120 GeV and up to 600 GeV at the 95% CL.

The significance of the excess of events observed in the previous combination, in the low mass range, decreases to, at most approximately 2 standard deviations, corresponding to a probability for a fluctuation of the background at the percent level. Such a fluctuation in the entire searched Higgs boson mass range is highly likely.

References

[1] F. Englert and R. Brout, *Broken symmetry and the mass of gauge vector mesons*, Phys. Rev. Lett. **13** (1964) 321–323.

[2] P. W. Higgs, *Broken symmetries, massless particles and gauge fields*, Phys. Lett. **12** (1964) 132–133.

[3] P. W. Higgs, *Broken symmetries and the masses of gauge bosons*, Phys. Rev. Lett. **13** (1964) 508–509.

[4] G. Guralnik, C. Hagen, and T. Kibble, *Global conservation laws and massless particles*, Phys. Rev. Lett. **13** (1964) 585–587.

[5] P. W. Higgs, *Spontaneous symmetry breakdown without massless bosons*, Phys. Rev. **145** (1966) 1156–1163.

[6] T. Kibble, *Symmetry breaking in non-Abelian gauge theories*, Phys. Rev. **155** (1967) 1554–1561.

[7] ATLAS Collaboration, *Combination of the Searches for the Higgs Boson in $\sim$1 fb^{-1} of Data Taken with the ATLAS Detector at 7 TeV Center-of-Mass Energy*, ATLAS-CONF-2011-112 (2011) .

[8] ATLAS Collaboration and CMS Collaboration, *LHC Higgs Combination Working Group Report*, ATL-PHYS-PUB-2011-818 (2011) .

[9] ATLAS Collaboration, *Search for neutral MSSM Higgs bosons decaying to tau+tau- pairs in proton-proton collisions at $\sqrt{s} = 7$ TeV with the ATLAS detector*, ATLAS-CONF-2011-132 (2011) .

[10] ATLAS Collaboration, *Search for the Standard Model Higgs boson in the decay mode $H \to \tau^+\tau^- \to \ell\ell + 4\nu$ in Association with jets in Proton-Proton Collisions at $\sqrt{s} = 7$ TeV with the ATLAS detector*, in preparation (2011) .

[11] ATLAS Collaboration, *Search for the Higgs boson in the two photon decay channel with the ATLAS detector at the LHC*, in preparation (2011) .

[12] ATLAS Collaboration, *Search for the Standard Model Higgs boson decaying to a b-quark pair with the ATLAS detector at the LHC*, ATLAS-CONF-2011-103 (2011) .

[13] ATLAS Collaboration, *Search for the Higgs boson in the $H \to WW^{(*)} \to \ell\nu\ell\nu$ decay mode with the ATLAS Detector*, in preparation .

[14] ATLAS Collaboration, *Search for the Standard Model Higgs boson in the decay channel $H \to ZZ^{(*)} \to \ell\ell\ell\ell$ with 1 fb^{-1} of pp collisions at $\sqrt{s} = 7$ TeV*, in preparation (2011) .

[15] ATLAS Collaboration, *Search for a Standard Model Higgs boson in the mass range 200-600 GeV in the $H \to ZZ \to \ell\ell\nu\nu$ final state with the ATLAS Detector*, in preparation (2011) .

[16] ATLAS Collaboration, *Search for a heavy Standard Model Higgs boson in the channel $H \to ZZ \to \ell\ell qq$ using the ATLAS detector*, in preparation (2011) .

[17] ATLAS Collaboration, *Commissioning of the ATLAS high-performance b-tagging algorithms in the 7 TeV collision data*, ATLAS-CONF-2011-102 (2011) .

[18] A. Elagin, P. Murat, A. Pranko, and A. Safonov, *A New Mass Reconstruction Technique for Resonances Decaying to di-tau*, `arXiv:1012.4686 [hep-ex]`.

[19] ATLAS Collaboration, *Limits on the production of the Standard Model Higgs Boson in pp collisions at $\sqrt{s} = 7$ TeV with the ATLAS detector*, `arXiv:1106.2748 [hep-ex]`.

[20] ATLAS Collaboration, *Search for Higgs Boson Production in pp Collisions at $\sqrt{s} = 7$ TeV using the $H \to WW \to \ell\nu qq$ Decay Channel and the ATLAS Detector*, in preparation (2011) .

[21] LHC Higgs Cross Section Working Group, S. Dittmaier, C. Mariotti, G. Passarino, and R. Tanaka (Eds.), *Handbook of LHC Higgs cross sections: 1. Inclusive observables*, CERN-2011-002 (CERN, Geneva, 2011) , `arXiv:1101.0593 [hep-ph]`.

[22] M. Botje, J. Butterworth, A. Cooper-Sarkar, A. de Roeck, J. Feltesse, et al., *The PDF4LHC Working Group Interim Recommendations*, `arXiv:1101.0538 [hep-ph]`.

[23] G. Cowan, K. Cranmer, E. Gross and O. Vitells, *Asymptotic formulae for likelihood-based tests of new physics*, Eur. Phys. J. **C71** (2011) 1–19.

[24] A. L. Read, *Modified frequentist analysis of search results (the CL_s method)*. http://cdsweb.cern.ch/record/451614/files/p81.pdf.

[25] A. L. Read, *Presentation of search results: The CL(s) technique*, J. Phys. **G28** (2002) 2693–2704.

[26] E. Gross and O. Vitells, *Trial factors for the look elsewhere effect in high energy physics*, The European Physical Journal C - Particles and Fields **70** (2010) 525–530.

[27] G. D. Kribs, T. Plehn, M. Spannowsky, and T. M. P. Tait, *Four generations and Higgs physics*, Phys. Rev. **D76** (2007) 075016.

[28] The CDF Collaboration, The D0 Collaboration, The Tevatron New Phenomena Higgs Working Group Collaboration, , t. D. Collaboration, t. T. N. Phenomena, and H. W. Group, *Combined CDF and D0 upper limits on $gg \to H \to W^+W^-$ and constraints on the Higgs boson mass in fourth-generation fermion models with up to 8.2 fb^{-1} of data*, `arXiv:1108.3331 [hep-ex]`.

[29] CMS Collaboration Collaboration, *Serch for the Standard Model Higgs boson in pp Collisions at $\sqrt{s} = 7$ TeV*, CMS-PAS-Hig-2011-011 (2011) .

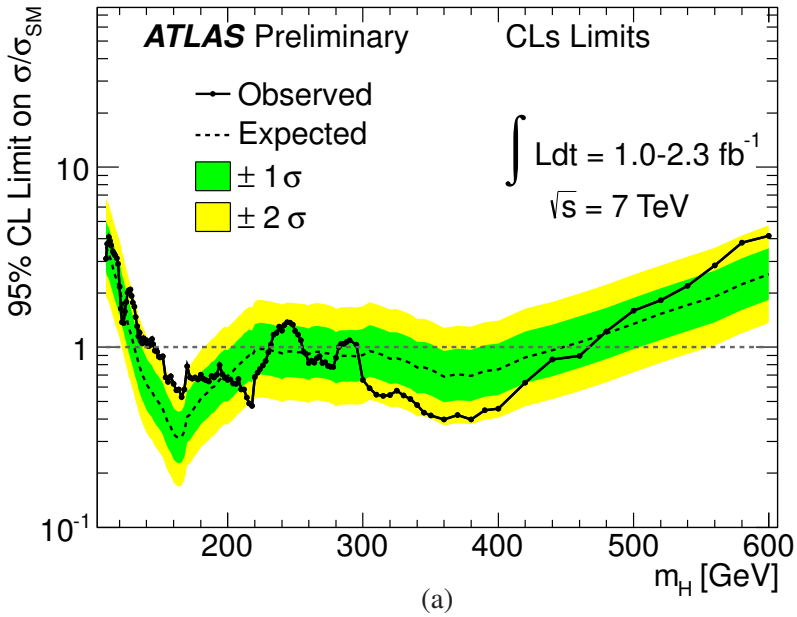

(a)

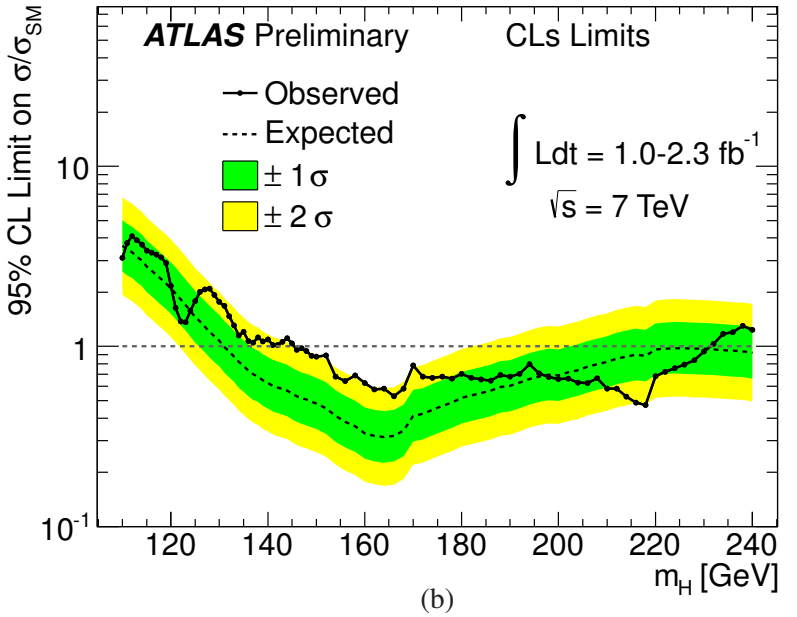

(b)

Figure 4: The combined upper limit on the Standard Model Higgs boson production cross section divided by the Standard Model expectation as a function of m_H is indicated by the solid line. This is a 95% CL limit using the CL_s method in the full mass range of this analysis (a) and in the low mass range (b). The dotted line shows the median expected limit in the absence of a signal and the green and yellow bands indicate the corresponding 68% and 95% expected regions.

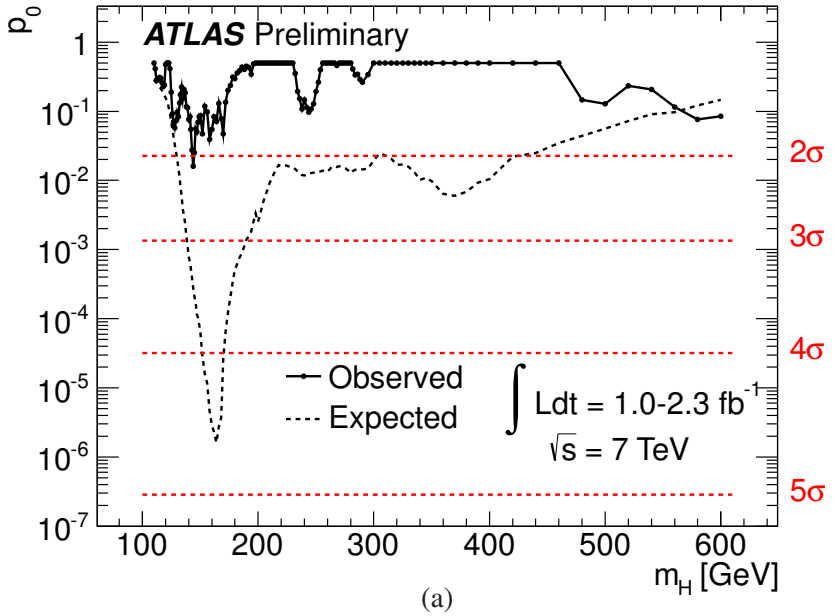

(a)

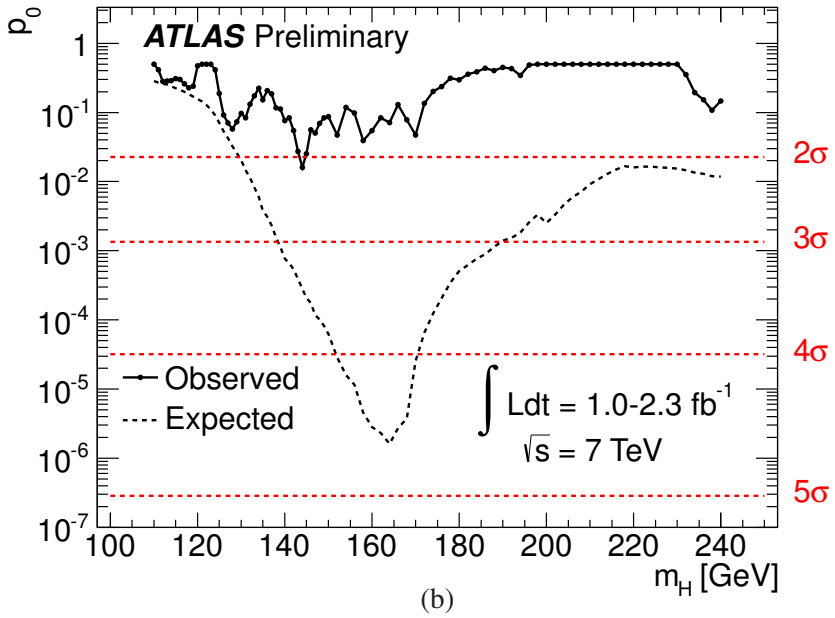

(b)

Figure 5: The consistency of the observed results with the background-only hypothesis is shown in the full mass range of this analysis (a) and in the low mass range (b). The noticeable excesses at 127 GeV, 144 GeV and 245 GeV reported in Ref. [7], are less significant but still present. The dashed line shows the median expected significance in the hypothesis of a Standard Model Higgs boson production signal. The four horizontal dashed lines indicate the p-values corresponding to significances of 2σ, 3σ, 4σ and 5σ.

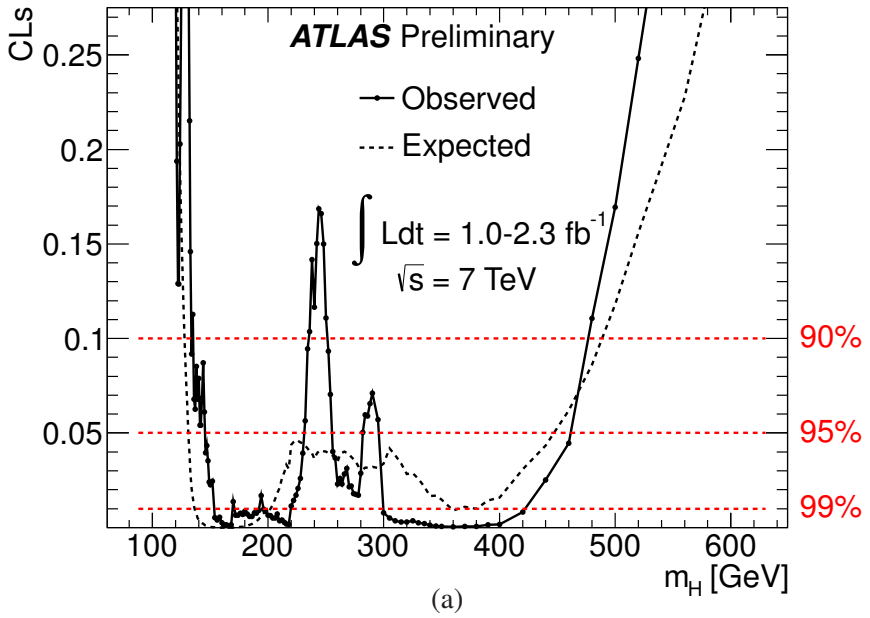

(a)

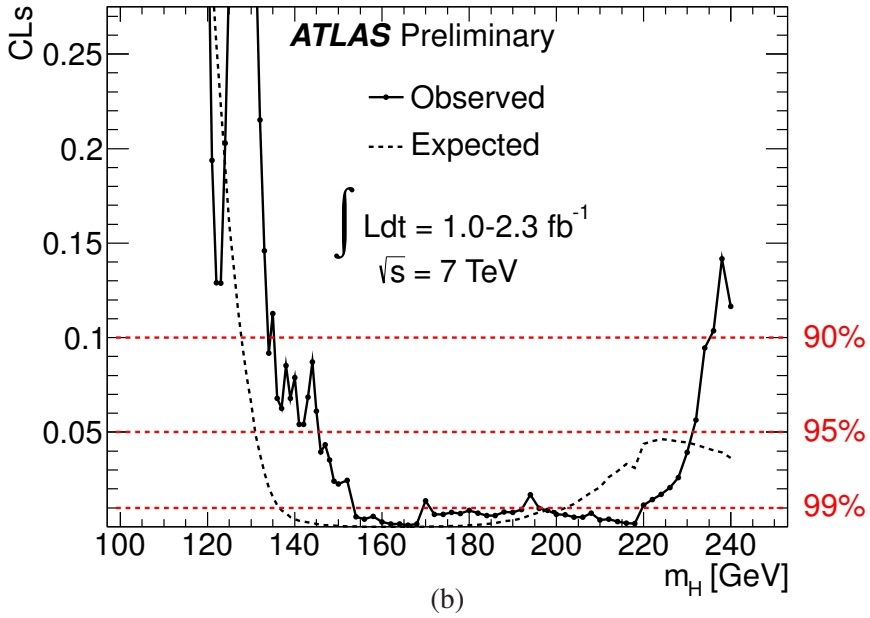

(b)

Figure 6: The value of the combined CL_s for $= 1$ (testing the Standard Model Higgs boson hypothesis) as a function of m_H in the full mass range of this analysis (a) and in the low mass range (b). By definition, the regions with $CL_s < \alpha$ are considered excluded at the $(1 - \alpha)$ CL or stronger.

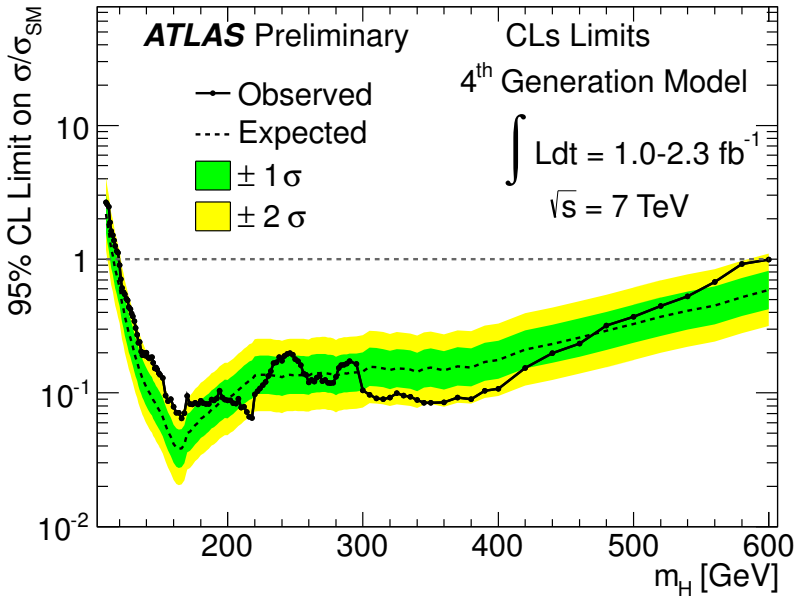

Figure 7: The combined upper limit on the Higgs boson production cross section in the framework of a Standard Model with the addition of a heavy fourth generation of fermions divided by its expectation as a function of m_H is indicated by the solid line. This is a 95% CL limit using the CL_s method. The dotted line shows the median expected limit in the absence of a signal and the green and yellow bands reflect the corresponding 68% and 95% expected regions.

Appendix A - $H \to \tau^+\tau^-$ Channels Combination

The $H \to \tau\tau \to \ell\tau_{had}3\nu$ and $H \to \tau\tau \to \ell^+\ell^- + 4\nu$ analyses are done in two different frameworks. The latter is an independent search for the Standard Model Higgs boson [10] and the former is part of the search for the Minimal Supersymmetric Standard Model Higgs boson, done in conjunction with other search channels [9]. The combination of these two search channels is done only in this note and illustrated in Fig. 3. To support this combination and illustrate its effect, the individual channels limits on the cross section normalised to the Standard Model Higgs boson cross section, as functions of the Higgs boson mass and their combination are illustrated in Fig. 8(a). The combination with the $\pm 1\sigma$ and $\pm 2\sigma$ variations of the background only expectation is illustrated in Fig. 8(b). As can be seen in Fig. 1(e) in the $H \to \tau\tau \to \ell\tau_{had}3\nu$ channel a deficit of events is observed mostly in the low mass range. The individual observed limit is therefore more stringent than the expected exclusion. A slight deficit of events is also observed in the $H \to \tau\tau \to \ell^+\ell^- + 4\nu$ channel as reported in Table 2. As the $H \to \tau\tau \to \ell\tau_{had}3\nu$ channel is significantly more sensitive than the $H \to \tau\tau \to \ell^+\ell^- + 4\nu$ channel, the combination differs only very slightly from the $H \to \tau\tau \to \ell\tau_{had}3\nu$ channel alone. It can be noted that the $H \to \tau^+\tau^-$ channels are only considered above 110 GeV for the overall combination.

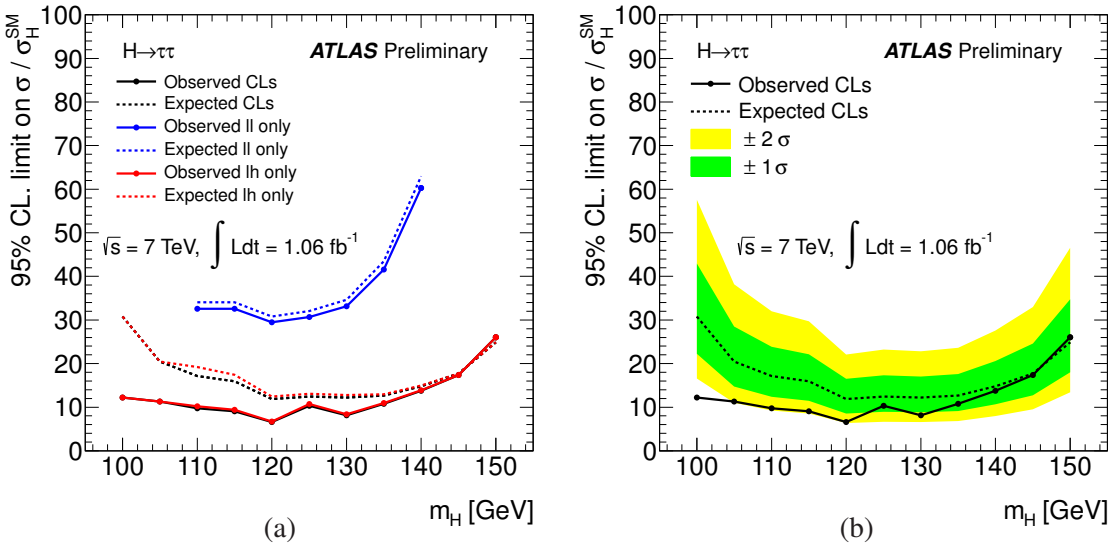

Figure 8: The observed and expected 95% CL upper limit using the CL_s method, on the Standard Model Higgs boson production cross section divided by the Standard Model expectation as a function of m_H for the individual $H \to \tau\tau \to \ell\tau_{had}3\nu$ and $H \to \tau\tau \to \ell^+\ell^- + 4\nu$ channels and their combination (a). The $H \to \tau^+\tau^-$ combined observed and expected 95% CL upper limits using the CL_s method (b). The green and yellow bands reflect the $\pm 1\sigma$ and $\pm 2\sigma$ variation respectively.

Appendix B - Results Summary

Table 4: The observed and expected CL_s, the observed and expected 95% CL upper limit on the Standard Model Higgs boson production cross section normalised to the Standard Model values using the CL_s method, and the p_0 for a set of Higgs boson mass hypotheses.

m_H(GeV)	CL_s		CL_s limits				p-values
	Obs.	Exp.	Obs.	-1σ	Median	+1σ	$p_{=0}$
110	0.473	0.558	3.11	2.6	3.62	5.03	0.5
111	0.609	0.543	3.76	2.48	3.45	4.8	0.412
112	0.678	0.526	4.1	2.4	3.33	4.63	0.281
113	0.649	0.504	3.88	2.27	3.16	4.39	0.284
114	0.626	0.483	3.67	2.16	3	4.17	0.289
115	0.586	0.454	3.4	2	2.78	3.86	0.308
116	0.574	0.428	3.31	1.9	2.63	3.67	0.299
117	0.584	0.403	3.23	1.8	2.5	3.47	0.258
118	0.587	0.378	3.12	1.7	2.36	3.28	0.228
119	0.551	0.351	2.9	1.61	2.23	3.11	0.24
120	0.346	0.324	2.17	1.52	2.11	2.93	0.474
121	0.194	0.291	1.64	1.42	1.97	2.74	0.5
122	0.129	0.255	1.38	1.31	1.82	2.53	0.5
123	0.129	0.223	1.37	1.22	1.7	2.36	0.5
124	0.203	0.19	1.58	1.13	1.57	2.19	0.413
125	0.295	0.16	1.79	1.05	1.46	2.03	0.187
126	0.338	0.138	2.01	0.989	1.37	1.91	0.0921
127	0.469	0.115	2.07	0.926	1.28	1.79	0.0706
128	0.49	0.0957	2.09	0.868	1.21	1.68	0.0574
129	0.43	0.0791	1.93	0.819	1.14	1.58	0.0729
130	0.362	0.0654	1.77	0.776	1.08	1.5	0.0969
131	0.315	0.0485	1.68	0.717	0.993	1.38	0.0839
132	0.215	0.0383	1.47	0.674	0.937	1.3	0.131
133	0.146	0.0288	1.31	0.634	0.879	1.23	0.173
134	0.0917	0.0207	1.15	0.59	0.82	1.14	0.225
135	0.113	0.0158	1.21	0.561	0.779	1.08	0.153
136	0.0678	0.0115	1.07	0.53	0.736	1.02	0.206
137	0.0627	0.00866	1.05	0.506	0.702	0.977	0.186
138	0.0852	0.00707	1.12	0.492	0.68	0.95	0.116
139	0.0678	0.00507	1.06	0.468	0.648	0.903	0.111
140	0.0789	0.00408	1.09	0.452	0.628	0.873	0.0762
141	0.0542	0.00313	1.02	0.436	0.606	0.842	0.0837
142	0.0541	0.00272	1.02	0.427	0.593	0.824	0.0545
143	0.0685	0.00233	1.06	0.418	0.581	0.807	0.0274
144	0.0872	0.00203	1.11	0.41	0.57	0.792	0.016

m_H(GeV)	CL_s		CL_s limits				p-values
	Obs.	Exp.	Obs.	-1σ	Median	+1σ	$p_{=0}$
145	0.0611	0.00147	1.04	0.394	0.547	0.761	0.0253
146	0.0396	0.00109	0.96	0.381	0.529	0.736	0.056
147	0.0434	0.000881	0.975	0.371	0.516	0.717	0.0505
148	0.0353	0.000752	0.943	0.365	0.507	0.704	0.0691
149	0.0241	0.000566	0.886	0.355	0.492	0.685	0.0835
150	0.0226	0.000473	0.879	0.347	0.482	0.67	0.087
152	0.0244	0.000255	0.893	0.327	0.455	0.632	0.0472
154	0.00532	7.59e-05	0.68	0.296	0.411	0.571	0.119
156	0.00406	2.83e-05	0.641	0.275	0.382	0.531	0.0987
158	0.00535	1.3e-05	0.69	0.26	0.36	0.501	0.039
160	0.00244	3.42e-06	0.625	0.238	0.33	0.459	0.0544
162	0.00139	2.28e-06	0.577	0.23	0.319	0.445	0.0837
164	0.00142	1.98e-06	0.582	0.226	0.314	0.437	0.0717
166	0.000796	2.38e-06	0.529	0.23	0.319	0.444	0.13
168	0.00152	6.52e-06	0.583	0.246	0.34	0.475	0.0781
170	0.0138	6.03e-05	0.783	0.297	0.412	0.573	0.0474
172	0.00652	8.31e-05	0.68	0.304	0.422	0.587	0.136
174	0.00662	0.00015	0.668	0.32	0.444	0.619	0.203
176	0.00748	0.000277	0.681	0.337	0.468	0.65	0.235
178	0.00684	0.000431	0.662	0.353	0.489	0.682	0.311
180	0.00866	0.000778	0.704	0.373	0.519	0.721	0.296
182	0.00724	0.00103	0.669	0.385	0.534	0.744	0.355
184	0.00586	0.00146	0.655	0.397	0.552	0.768	0.387
186	0.00581	0.00193	0.647	0.41	0.569	0.791	0.436
188	0.00779	0.00287	0.693	0.429	0.595	0.828	0.402
190	0.00761	0.0033	0.679	0.435	0.604	0.84	0.445
192	0.00908	0.00445	0.706	0.454	0.63	0.876	0.43
194	0.0169	0.00615	0.798	0.476	0.659	0.919	0.344
196	0.0097	0.00757	0.706	0.492	0.681	0.95	0.488
198	0.0086	0.00877	0.677	0.502	0.697	0.97	0.5
200	0.00661	0.00792	0.659	0.498	0.691	0.962	0.5
202	0.00624	0.00998	0.661	0.517	0.717	0.998	0.5
204	0.00499	0.0121	0.629	0.532	0.738	1.03	0.5
206	0.00512	0.0152	0.627	0.555	0.771	1.07	0.5
208	0.00707	0.0181	0.667	0.573	0.796	1.11	0.5
210	0.00363	0.021	0.583	0.59	0.819	1.14	0.5
212	0.00405	0.0261	0.583	0.616	0.856	1.19	0.5
214	0.00264	0.0294	0.527	0.633	0.878	1.22	0.5

m_H(GeV)	CL_s		CL_s limits				p-values
	Obs.	Exp.	Obs.	-1σ	Median	+1σ	$p_{=0}$
216	0.0019	0.0331	0.487	0.65	0.902	1.25	0.5
218	0.00174	0.031	0.473	0.639	0.887	1.23	0.5
220	0.0115	0.0437	0.683	0.695	0.965	1.34	0.5
222	0.0144	0.0452	0.721	0.704	0.973	1.36	0.5
224	0.017	0.0463	0.756	0.708	0.98	1.37	0.5
226	0.0207	0.0458	0.794	0.706	0.977	1.36	0.5
228	0.026	0.0451	0.838	0.7	0.972	1.35	0.5
230	0.0393	0.0446	0.94	0.699	0.97	1.35	0.5
232	0.0564	0.0434	1.03	0.694	0.963	1.34	0.352
234	0.0945	0.0419	1.18	0.687	0.955	1.33	0.194
236	0.104	0.0404	1.2	0.681	0.946	1.32	0.152
238	0.142	0.0394	1.3	0.677	0.94	1.31	0.107
240	0.116	0.0364	1.24	0.664	0.923	1.28	0.145
242	0.15	0.0391	1.33	0.675	0.938	1.3	0.114
244	0.169	0.0404	1.37	0.682	0.947	1.32	0.0972
246	0.166	0.0408	1.37	0.683	0.949	1.32	0.108
248	0.15	0.0403	1.34	0.681	0.946	1.31	0.128
250	0.111	0.0401	1.23	0.68	0.945	1.31	0.194
252	0.0934	0.0393	1.17	0.676	0.939	1.31	0.263
254	0.0703	0.0387	1.1	0.674	0.936	1.3	0.397
256	0.0402	0.0381	0.943	0.671	0.933	1.3	0.5
258	0.0368	0.0364	0.921	0.664	0.923	1.28	0.5
260	0.0231	0.0349	0.818	0.657	0.913	1.27	0.5
262	0.0259	0.0386	0.845	0.674	0.936	1.3	0.5
264	0.023	0.0396	0.821	0.678	0.942	1.31	0.5
266	0.0283	0.0402	0.869	0.68	0.945	1.31	0.5
268	0.0312	0.0394	0.892	0.678	0.941	1.31	0.458
270	0.0215	0.0386	0.817	0.674	0.937	1.3	0.5
272	0.0219	0.0375	0.824	0.669	0.929	1.29	0.5
274	0.0179	0.0362	0.787	0.664	0.922	1.28	0.5
276	0.0175	0.0346	0.78	0.657	0.913	1.27	0.5
278	0.0171	0.0324	0.775	0.647	0.899	1.25	0.5
280	0.0288	0.0278	0.874	0.628	0.87	1.21	0.5
282	0.0503	0.0307	1	0.641	0.889	1.24	0.406
284	0.0596	0.0316	1.05	0.644	0.894	1.24	0.335
286	0.0589	0.0317	1.04	0.645	0.895	1.25	0.342
288	0.0656	0.0317	1.07	0.644	0.894	1.24	0.29
290	0.0711	0.0322	1.09	0.646	0.897	1.25	0.264

m_H(GeV)	CL_s		CL_s limits				p-values
	Obs.	Exp.	Obs.	-1σ	Median	+1σ	$p_{=0}$
295	0.057	0.0316	1.03	0.643	0.893	1.24	0.339
300	0.00771	0.0338	0.661	0.652	0.906	1.26	0.5
305	0.00505	0.0419	0.591	0.686	0.953	1.33	0.5
310	0.00345	0.0383	0.547	0.67	0.931	1.29	0.5
315	0.00288	0.0338	0.536	0.65	0.903	1.26	0.5
320	0.00282	0.0284	0.544	0.626	0.866	1.21	0.5
325	0.00355	0.0287	0.573	0.628	0.871	1.21	0.5
330	0.00253	0.0258	0.539	0.61	0.846	1.18	0.5
335	0.00203	0.0215	0.514	0.588	0.816	1.14	0.5
340	0.00126	0.0166	0.477	0.555	0.771	1.07	0.5
345	0.000756	0.0168	0.434	0.556	0.772	1.07	0.5
350	0.000597	0.0148	0.418	0.541	0.752	1.04	0.5
360	0.000377	0.00898	0.397	0.494	0.685	0.955	0.5
370	0.000657	0.0109	0.42	0.509	0.707	0.983	0.5
380	0.000564	0.00987	0.398	0.502	0.694	0.969	0.5
390	0.00134	0.0144	0.448	0.532	0.739	1.03	0.5
400	0.00158	0.0159	0.456	0.543	0.754	1.05	0.5
420	0.00811	0.0308	0.637	0.633	0.878	1.22	0.5
440	0.0251	0.0434	0.857	0.691	0.96	1.34	0.5
460	0.0445	0.0621	0.897	0.769	1.07	1.48	0.5
480	0.111	0.0861	1.22	0.859	1.19	1.66	0.146
500	0.169	0.118	1.6	0.975	1.35	1.88	0.128
520	0.248	0.156	1.82	1.1	1.53	2.13	0.234
540	0.326	0.192	2.19	1.23	1.71	2.38	0.208
560	0.473	0.228	2.84	1.38	1.91	2.66	0.115
580	0.583	0.284	3.81	1.61	2.23	3.12	0.0764
600	0.6	0.334	4.16	1.83	2.54	3.54	0.0843